Stabilization of Traffic Flow Based on the Multiple Information of Preceding Cars

D. F. Xie[1,2,*], Z. Y. Gao[1,2] and X. M. Zhao[2]

[1] *State Key Laboratory of Rail Traffic Control and Safety, Beijing Jiaotong University, Beijing 100044, China.*
[2] *Institute of System Science, School of Traffic and Transportation, Beijing Jiaotong University, Beijing 100044, China.*

Abstract. To enhance the stability of traffic flow, a new car-following model is proposed by taking into account the support of intelligent transportation system (ITS) information, which includes both the headway and the velocity difference of multiple preceding cars. The new model is based on the Optimal Velocity (OV) model and its extended models. The stability condition of the model is obtained by using the linear stability theory. Through nonlinear analysis, the modified Korteweg-de Vries equation is constructed and solved, and the traffic flow is classified into three types, i.e. stable, metastable, and unstable. The jam phase can thus be described by the kink-antikink soliton solution for the mKdV equation. The numerical simulation results show that compared with previous models considering only one of the ITS information, the proposed model can suppress traffic jams more efficiently when both headway and velocity difference of arbitrary preceding cars are taken into account. The results of numerical simulation coincide with the theoretical ones.

1 Introduction

Traffic phenomena have attracted much attention from physicists in recent years. Many studies have been conducted with different traffic models, such as the cellular automaton models, car-following models, hydrodynamic models and gas kinetic models [1, 2]. The

---

*Corresponding author. *Email addresses:* dongfanxie@gmail.com (D. F. Xie), zygao@center.bjtu.edu.cn (Z. Y. Gao), zhaoxiaomei@jtys.bjtu.edu.cn (X. M. Zhao)

car-following model is one of the most important microscopic models that depict the motion of cars by differential equations. In 1995, Bando et al. [3] proposed the optimal velocity (OV) model which can describe many nonlinear characteristics of traffic flow, such as nonequilibrium traffic flow, jam formation and stop and go waves, and thus attracted much attention [4–7]. Generally, it is important to enhance the stability of traffic flow to avoid traffic jams.

Recently, with the development of the intelligent transportation system (ITS), the traffic control system has been utilized as a part of ITS, and drivers can receive information of other cars on the roads. Several traffic flow models have been proposed involving the use of ITS information [8–15] to enhance the stability of traffic flow. Nagatani [8] presented an extended car following model by taking into account the car interaction of before the next car ahead. Nakayama et al. [9] discussed the improvement of stability when a driver looks at the car that follows. Lenz et al. [10] extended the OV model by incorporating interactions of multiple cars ahead. Ge et al. [12–14] presented another car following model that incorporates the headways of arbitrary preceding cars. Hasebe et al. [11] proposed a fully extended OV model by taking into account the information of arbitrary cars that precede or follow. However, all of the above models considered only the interactions induced by the headways. On the other hand, based on the full velocity difference (FVD) model [5] (which is an extended OV model by introducing the velocity difference term), Wang et al. [15] presented the multiple velocity difference (MVD) model to improve the stability of traffic flow.

Previous studies indicate that the headway or velocity difference can stabilize the traffic flow. However, all existing models are only subject to one type of the ITS information, either headway or velocity difference of other cars. It is expected that the traffic flow can be more stable by simultaneously introducing both two types of the ITS information. Thus based on the OV model and its related models, an extended car-following model by incorporating both headways and velocity difference of multiple preceding cars, called multiple headway and velocity difference (MHVD) model, is presented in this paper. We then give the stability condition of the model by using the linear stability theory. Moreover, the nonlinear analysis is applied to derive the modified Korteweg-de Vries (mKdV) equation near the critical point, and its kink-antikink soliton solution to describe the traffic jam is also obtained. Numerical simulation is carried out to validate the theoretical analysis. Comparisons between previous models considering only one type of the ITS information and the proposed model here are made. The results show that in our model the stability of traffic flow is clearly enhanced when multiple ITS information is considered.

This paper is organized as follows: in Section 2, the OV model and two of its extended models are reviewed, and the MHVD model is presented. In Section 3 linear stability analysis is applied to the MHVD model. Nonlinear analysis of the model is given in Section 4. The property of our model is investigated using numerical methods in Section 5. Conclusions are summarized in the final section.

2   Models

It is necessary to review the optimal velocity (OV) model and some of its extended models before presenting the new model. The dynamic equation of the OV model is [3],

$$\frac{d^2x_n(t)}{dt^2} = a[V(\Delta x_n(t)) - v_n(t)], \qquad (n=1,2,\cdots,N), \tag{2.1}$$

where $x_n(t)$ and $x_{n+1}(t)$ are the positions of cars n and its front car $n+1$ at time t,

$$\Delta x_n(t) = x_{n+1}(t) - x_n(t)$$

is the headway of car n, $v_n(t) = dx_n(t)/dt$ is the velocity of car n, $V(\cdot)$ is the optimal velocity function, a is the sensitivity parameter, and N is the total car number on the road. With the development of new technologies, Hasebe et al. [11] proposed an extended OV model applicable to cooperative driving control system incorporating the headway information of arbitrary number of cars that precede or follow. The model is formulated as,

$$\frac{d^2x_n(t)}{dt^2} = a\Big[V(\Delta x_{n+p_+}(t),\cdots,\Delta x_{n+1}(t),\Delta x_n(t),\Delta x_{n-1}(t),\cdots,\Delta x_{n-p_-}(t)) - v_n(t)\Big], \tag{2.2}$$

where $\Delta x_{n+p_+}(t),\cdots,\Delta x_{n+1}(t)$ are headways of the cars ahead the n car, and $\Delta x_{n-1}(t),\cdots,$ $\Delta x_{n-p_-}(t)$ are headways of the cars that follow. The model with $p_+ = p_- = 0$ is the OV model. They pointed out that the headway information of preceding cars as well as the following ones can improve the stability of traffic flow.

Recently, based on the OV and its extended models, Wang et al. [15] proposed another car following model incorporating multiple velocity difference of preceding cars. The differential equation of the model is given as

$$\frac{d^2x_n(t)}{dt^2} = a[V(\Delta x_n(t)) - v_n(t)] + \sum_{j=1}^{q}\kappa_j\Delta v_{n+j-1}(t), \tag{2.3}$$

where

$$\Delta v_{n+j-1}(t) = v_{n+j}(t) - v_{n+j-1}(t),$$

and κ_j are the coefficients of velocity difference. They pointed out that the critical value of the sensitivity in the MVD model decreases and the stable region is apparently enlarged when the information of multiple preceding cars is considered.

The previous studies show that the headways or velocity difference can be helpful to enhance the stability of traffic flow. We expect that if both the information of multiple headway and velocity difference are used at the same time, then the stability of traffic can be further improved. Thus the multiple headway and velocity difference (MHVD) model is presented here. The differential equation is given as

$$\frac{d^2x_n(t)}{dt^2} = a\Big[V(\Delta x_n(t),\Delta x_{n+1}(t),\cdots,\Delta x_{n+p-1}(t)) - v_n(t)\Big] + \sum_{j=1}^{q}\kappa_j\Delta v_{n+j-1}(t), \tag{2.4}$$

where $a = 1/\tau$ is the sensitivity parameter, and $\kappa_j = \lambda_j/\tau$ is the coefficient of velocity difference, p and q are the number of preceding cars considered. Generally, p is equal to q. However, to compare with the previous works, we select them optionally in our model. The first term on the right side of Eq. (2.4) denotes stimulus to a driver about the difference between the optimal velocity and the current velocity, and the second term on the right side of Eq. (2.4) denotes stimulus to a driver about velocity difference of multiple preceding cars. In this paper, the boundary conditions are assumed to be periodic. The optimal velocity $V(\cdot)$ depending on the car headways is,

$$V(\Delta x_n(t),\Delta x_{n+1}(t),\cdots,\Delta x_{n+p-1}(t)) = V\left(\sum_{l=1}^{p}\beta_l\Delta x_{n+l-1}(t)\right), \tag{2.5}$$

where β_l is the weighted function of $\Delta x_{n+l-1}(t)$. It is assumed that β_l decreases with the increase of l, which means the effect of headway decreases with the increase of preceding car number. The optimal velocity function is selected similar to that in Ref. [3]:

$$V\left(\sum_{l=1}^{p}\beta_l\Delta x_{n+l-1}(t)\right) = \frac{1}{2}v_{\max}\left[\tanh\left(\sum_{l=1}^{p}\beta_l\Delta x_{n+l-1}(t) - h_c\right) + \tanh(h_c)\right], \tag{2.6}$$

where $v_{\max}$ is the maximal velocity, and h_c is the safety distance.

3   Linear stability analysis

The method of linear stability is applied to the MHVD model. Let $a_c(\theta)$ to be the critical value of a for the Fourier-mode $\exp(i\theta n + i\omega t)$, where $\theta = 2\pi k/N$, $(k = 0,1,2,\cdots,N-1)$, N is the total car number. It is (see the derivation in Appendix A)

$$a_c(\theta) = \omega^2\left[\omega\sum_{j=1}^{q}\lambda_j\left(\sin(\theta j) - \sin\theta(j-1)\right) - V'(h)\sum_{l=1}^{p}\beta_l\left(\cos(\theta l) - \cos\theta(l-1)\right)\right]^{-1}, \tag{3.1}$$

where h is the constant headway when the traffic flow is stable, and ω is

$$\omega = V'(h)\sum_{l=1}^{p}\beta_l\left(\sin(\theta l) - \sin\theta(l-1)\right)\left(1 - \sum_{j=1}^{q}\lambda_j\left(\cos(\theta j) - \cos\theta(j-1)\right)\right)^{-1}. \tag{3.2}$$

For the following analysis and numerical simulation, we take the parameters β_l (similar to Ge et al. [12]) and λ_j (similar to Li et al. [22]) of the MHVD model as

$$\beta_l = \begin{cases} \dfrac{6}{7^l} & l \neq p, \\[2mm] \dfrac{1}{7^{p-1}} & l = p, \end{cases} \tag{3.3}$$

and

$$\lambda_j = \lambda_0 (1/5)^j, \qquad (j=1,2,\cdots,q), \tag{3.4}$$

where

$$\sum_{l=1}^{p} \beta_l = 1, \qquad \beta_l = 1 \quad \text{for} \quad p=1,$$

λ_0 is a constant parameter. From numerical calculation of Eq. (3.1) with (3.3)-(3.4), it can be found that $a_c(\theta)$ reaches its maximum value as $\theta \to 0$. Thus the neutral stable line can be given as

$$a = 2V'(h) \left(\sum_{l=1}^{p} \beta_l (2l-1) + 2\sum_{j=1}^{q} \lambda_j \right)^{-1}. \tag{3.5}$$

For small disturbances of long wavelengths, the uniform traffic flow is stable if

$$a > 2V'(h) \left(\sum_{l=1}^{p} \beta_l (2l-1) + 2\sum_{j=1}^{q} \lambda_j \right)^{-1}. \tag{3.6}$$

When $\lambda_j = 0$, $(j=1,2,\cdots,q)$, the MHVD model is equal to the model proposed by Hasebe et al. [11] with $p_- = 0$ (where p_- is the number of behind cars), and Eq. (3.6) can be rewritten as

$$a > 2V'(h) \left(\sum_{l=1}^{p} \beta_l (2l-1) \right)^{-1}. \tag{3.7}$$

From Eqs. (3.6)-(3.7), it can be found that the stability region of the MHVD model is further enlarged when both two types of the ITS information are considered.

The MHVD model is simplified to the MVD model for $p=1$ and $\beta_l = 1$. In this case, Eq. (3.6) can be rewritten as

$$a > 2V'(h) \left(1 + 2\sum_{j=1}^{q} \lambda_j \right)^{-1}. \tag{3.8}$$

From Eqs. (3.6) and (3.8), it can be found that the stability condition of the MHVD model can be satisfied more easily than the MVD model, due to the introduction of the multiple ITS information.

The neutral stability curves in the parameter space $(\Delta x, a)$ are shown in Fig. 1. The curves are obtained based on Eq. (3.5), which are the critical boundaries of the linear stability regions. Obviously, there exist the critical points (a_c, h_c) for the neutral stability subject to different sets of (p,q). From Fig.1, it can be seen that the critical points and the neutral stability curves are lowered as the information of more preceding cars is taken into account, which means the stability condition of the uniform traffic flow has been strengthened. Assume that s denotes the number of cars taken into account. In the following, the cases with identical s will be compared. For $s=1$, the curve of $(p,q)=(1,1)$
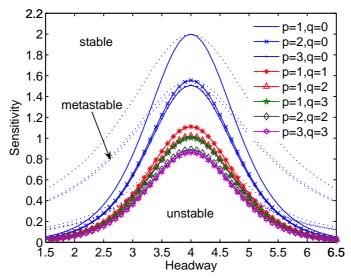
Figure 1: Phase diagram in the headway-sensitivity space. The solid lines represent neutral stability curves defined by Eq. (3.5) (which are the critical boundaries of the linear stable regions), and the dotted lines indicate the coexisting curves. For each set of (p,q), the plane is divided into three regions by the solid line and dotted line: stable region above the dotted line, metastable region between the solid line and the dotted line (metastable state is the state under that there exists a critical amplitude for the formation of traffic jams), and unstable region below the solid line. ($v_{\max}=2$, $h_c=4$, $\lambda_0=2$).

is below the curve of $(p,q)=(1,0)$, meaning that the case of considering both two types of information has more efficient effect on the traffic stability than that using only one of them when the same amount of preceding cars are taken into account. Compared with the cases of $s=2$, with for example $(p,q)=(2,2)$ and $(p,q)=(2,0)$, $(p,q)=(2,2)$ and $(p,q)=(1,2)$, and $s=3$, with for example $(p,q)=(3,3)$ and $(p,q)=(3,0)$, $(p,q)=(3,3)$ and $(p,q)=(1,3)$, similar results can be obtained.

4 Nonlinear analysis

In recent years, some researchers have investigated the traffic jam by using nonlinear analysis. Kurtz and Hong [16] derived the Korteweg-de Vries (KdV) equation from the hydrodynamic model and show that the traffic soliton appears near the neutral stability line. Komatsu and Sasa [17] deduced the modified KdV (mKdV) equation from the OV model proposed by Bando et al. [3]. Nagatani [18] derived the mKdV equation based on a hydrodynamic model. In [8], Nagatani also investigated a car following model by nonlinear analysis and derived the mKdV equation. Ge et al. [12] used the nonlinear analysis base on another car following model incorporating the ITS information. In this paper, the method of nonlinear analysis is applied to the MHVD model. Consequently, the slowly varying behavior for long waves in the stable and unstable regions can be obtained.

First, slow scales for the space variable n and the time variable t are introduced. Define the slow variable X and T as follows:

$$X = \varepsilon(n + bt), \tag{4.1}$$

$$T = \varepsilon^3 t, \tag{4.2}$$

where $0 < \varepsilon \ll 1$, b is a constant to be determined. Let

$$\Delta x_n(t) = h_c + \varepsilon R(X, T). \tag{4.3}$$

Substituting Eq. (2.6) into Eq. (2.4) and reorganizing the resulting equation gives

$$
\begin{aligned}
\frac{d^2(\Delta x(t))}{dt^2} = {} & a \left[V\left(\sum_{l=1}^{p} \beta_l \Delta x_{n+l}(t) \right) - V\left(\sum_{l=1}^{p} \beta_l \Delta x_{n+l-1}(t) \right) - \frac{d(\Delta x_n(t))}{dt} \right] \\
& + \sum_{j=1}^{q} \kappa_j \left[\frac{d(\Delta x_{n+j}(t))}{dt} - \frac{d(\Delta x_{n+j-1}(t))}{dt} \right].
\end{aligned}
\tag{4.4}
$$

Then from nonlinear analysis (see Appendix B), we obtain

$$\partial_T R' - \partial_X^3 R' + \partial_X R'^3 + \varepsilon M[R'] = 0, \tag{4.5}$$

where $T' = g_1 T$, $R = \sqrt{g_1/g_2} R'$, and

$$M[R'] = g_1^{-1/2} \left(g_3 \partial_X^2 R' + \frac{g_1 g_5}{g_2} \partial_X^2 R'^3 + g_4 \partial_X^4 R' \right), \tag{4.6}$$

where

$$V' = \frac{dV(\Delta x_n)}{d\Delta x_n} \bigg|_{\Delta x_n = h_c} = V'(h_c), \quad V''' = \frac{d^3 V(\Delta x_n)}{d\Delta x_n^3} \bigg|_{\Delta x_n = h_c} = V'''(h_c), \tag{4.7}$$

and

$$g_1 = \frac{1}{6} V' \sum_{l=1}^{p} \beta_l (3l^2 - 3l + 1) + \frac{1}{2} \sum_{j=1}^{q} \left(\kappa_j (2j - 1) V'/a_c \right), \tag{4.8a}$$

$$g_2 = -\frac{1}{6} V''', \quad g_3 = \frac{1}{2} V' \sum_{l-1}^{p} \beta_l (2l - 1), \tag{4.8b}$$

$$
\begin{aligned}
g_4 = {} & \left(\frac{2V'}{a_c} - \sum_{j=1}^{q} \frac{\kappa_j}{a_c} \right) \left[\frac{1}{6} V' \sum_{l=1}^{p} \beta_l (3l^2 - 3l + 1) + \frac{1}{2} \sum_{j=1}^{q} \left(\kappa_j (2j - 1) V'/a_c \right) \right] \\
& + \left[-\frac{1}{24} V' \sum_{l=1}^{p} \beta_l (4l^3 - 6l^2 + 4l - 1) - \frac{1}{6} \sum_{j=1}^{q} \kappa_j V' (3j^2 - 3j + 1)/a_c \right],
\end{aligned}
\tag{4.8c}
$$

$$g_5 = -\frac{1}{12} V''' \left(\sum_{l=1}^{p} \beta_l (2l - 1) - 4V'/a_c - 2 \sum_{j=1}^{q} \kappa_j \right). \tag{4.8d}$$

Eq. (4.5) is the modified KdV equation with an $o(\varepsilon)$ correction term. First, we ignore the $o(\varepsilon)$ term in Eq. (4.5) and get the mKdV equation with the kink-antikink soliton solution

$$R'_o(X,T') = \sqrt{c}\tanh\sqrt{\frac{c}{2}}(X-cT'), \tag{4.9}$$

where c is the propagation velocity. In order to determine c for the solution of Eq. (4.5), the following requirement must be satisfied:

$$(R'_o, M[R'_o]) = \int_{-\infty}^{+\infty} dX R'_o(X,T') M[R'_o(X,T')] = 0, \tag{4.10}$$

where $M[R'_o] = M[R']$. By solving the above equation, we obtain

$$c = 5g_2 g_3 / (2g_2 g_4 - 3g_1 g_5). \tag{4.11}$$

Hence, the kink-antikink soliton solution is of the form

$$R(X,T) = \left[\left(-V'\sum_{l=1}^{p}\beta_l(3l^2-3l+1)+3\sum_{j=1}^{q}\left(\kappa_j(2j-1)\frac{V'}{a_c}\right)\right)\frac{c}{V'''}\right]^{1/2}\tanh\sqrt{\frac{c}{2}}$$
$$\times\left[X-cT\left(\frac{1}{6}V'\sum_{l=1}^{p}\beta_l(3l^2-3l+1)+\frac{1}{2}\sum_{j=1}^{q}\left(\kappa_j(2j-1)\frac{V'}{a_c}\right)\right)\right]. \tag{4.12}$$

Here the amplitude A of the solution is

$$A = \left(\left(\frac{a_c}{a}-1\right)\left[V'\sum_{l=1}^{p}\beta_l(3l^3-3l+1)+3\sum_{j=1}^{q}\left(\kappa_j(2j-1)\frac{V'}{a_c}\right)\right]\frac{c}{-V'''}\right)^{1/2}, \tag{4.13}$$

where

$$a_c = \left(2V'(h_c)-2\sum_{j=1}^{q}\kappa_j\right)\left(\sum_{l=1}^{p}\beta_l(2l-1)\right)^{-1}.$$

The kink solution represents the coexisting phase which includes both freely moving phase and jamming phase, and the headways of the two phases are given by $\Delta x = h_c + A$ and $\Delta x = h_c - A$, respectively. According to these, we can depict the coexisting curves in the plane $(\Delta x, a)$, as shown by dotted lines in Fig. 1.

Fig. 1 is the phase diagram in the headway-sensitivity space. For each set of (p,q), the plane is divided into three regions by the solid line (representing the neutral stability curve) and the dotted line (representing the coexisting curve): the part above the dotted line is the stable region, the part between the solid line and the dotted line is the metastable region, and the part below the solid line is the unstable region. From Fig. 1, it can be seen that both the neutral stability curve and the coexisting curve decrease with
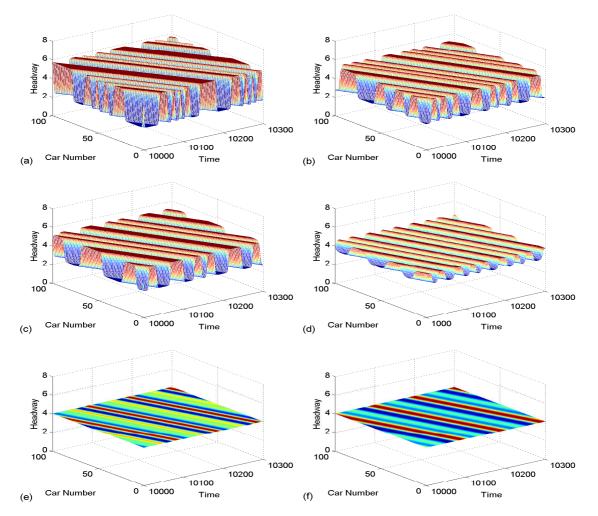
Figure 2: Space-time evolution of the headways after $t = 10000s$. The patterns (a)-(f) are for the coexisting phases which corresponding to the cases of $(p,q) = (1,0)$, $(2,0)$, $(3,0)$, $(1,1)$, $(1,2)$ and $(1,3)$ respectively.

the increase of p or q, which means the stable regions are enlarged, and the unstable regions are reduced when the information of more preceding cars are taken into account. In addition, the cases with identical s (which is the number of cars taken into account) will be compared in the following. Compared with $(p,q) = (1,1)$ and $(p,q) = (1,0)$, it can be seen that both the neutral stability curve and the coexisting curve are decreased, meaning that the stable region is enlarged, and the unstable region is reduced; compared with $(p,q) = (2,2)$ and $(p,q) = (2,0)$, $(p,q) = (2,2)$ and $(p,q) = (1,2)$, $(p,q) = (3,3)$ and $(p,q) = (3,0)$, $(p,q) = (3,3)$ and $(p,q) = (1,3)$, the same results can be obtained. We can thus conclude that the case considering both types of the ITS information has a more efficient effect on the traffic stability than that considering only one of them.
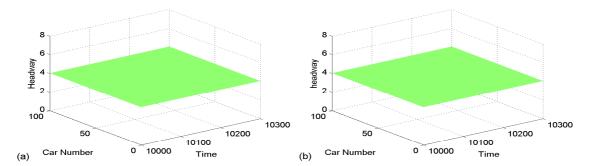
Figure 3: Space-time evolution of the headways after $t=10000s$. The patterns are for freely moving phase corresponding to the cases of $(p,q)=(2,2)$ and $(3,3)$ respectively.

5 Numerical results

In this section, to validate the results of the theoretical analysis, numerical simulation is carried out for the MHVD model described by Eq. (2.4). The periodical boundary conditions are used. The initial conditions are given as follows: $\Delta x=4$ for $n\neq 50,51$, $\Delta x=4-0.5$ for $n=50$, and $\Delta x=4+0.5$ for $n=51$, where the total number of cars is $N=100$. The safety distance is $h_c=4$, and other input parameters are $a=1.0$, $\lambda_0=2$, $v_{\max}=2$. According to the results of the stability analysis above, the traffic flow is unstable when $(p,q)=(1,0), (2,0), (3,0), (1,1), (1,2)$ and $(1,3)$; and is stable when $(p,q)=(2,2)$ and $(3,3)$.

Fig. 2 shows the space-time evolution of the headways for different sets of (p,q). In Fig. 2, the traffic flow is unstable because the stability condition Eq. (3.6) is unsatisfied. When small disturbances are added to the uniform traffic flow, they are amplified with time and the uniform flow changes finally to inhomogeneous traffic flow.

In Fig. 3, the disturbances disappear and the traffic flow becomes uniform over the whole space. In addition, for fixed $q=0$, the traffic jams abate gradually for Fig. 2 (a)-(c) with the increase values of p; similarly, for fixed $p=1$, the traffic jams abate obviously for Fig. 2 (d)-(f) with the increase values of q. Furthermore, the traffic jams completely disappear for Fig. 3. It thus can be concluded that the traffic jam can be suppressed more effectively by taking into account both ITS information of headway and velocity difference than by considering only one of them. In Fig. 2, the kink-antikink soliton solution appears as traffic jam and the density waves propagate backwards. The simulation results are in good agreement with the analytical ones.

6 Summary

Based on the OV model and its extended models, the multiple headway and velocity difference (MHVD) model has been proposed by considering the multiple ITS information. The traffic nature has been analyzed analytically by using the linear and nonlinear

analysis. The mKdV equation has been derived to describe the traffic behavior near the critical point, and the traffic flows are classified into three types, i.e., stable, metastable, and unstable. Obviously, the stable region is enlarged by taking into account the multiple ITS information of preceding cars. The simulation results show that the traffic jams can be suppressed more effectively in our model with both ITS information of headway and velocity difference than those with only one of them, which are in good agreement with the analytical ones.

Of course, it will take a long time for the cars to use ITS widely, and the mixed traffic flow consisting of intelligent cars and usual cars will be last for a long period. For this reason, further study on the mixed traffic flow is needed [20, 21].

Acknowledgments

A   Appendix to Section 3

Here we derive some formulas given in Section 3. Substituting Eq. (2.5) into Eq. (2.4), we rewrite the resulting equation as

$$\frac{d^2 x_n(t)}{dt^2} = a\left[V\left(\sum_{l=1}^{p}\beta_l \Delta x_{n+l-1}(t)\right) - v_n(t)\right] + \sum_{j=1}^{q}\kappa_j \Delta v_{n+j-1}(t). \qquad (A.1)$$

It is obvious that the uniform traffic flow, i.e., the car moves with constant headway and the optimal velocity $V(h,h,\cdots,h)$, is the steady-state solution of Eq. (2.4), given by

$$x_n^0(t) = hn + V(h,h,\cdots,h)t \qquad \text{with} \qquad h = L/N, \qquad (A.2)$$

where N is the total number of cars, and L is the road length. Suppose $y_n(t)$ is a small deviation from the steady-state solution $x_n^0(t)$, i.e.,

$$x_n(t) = x_n^0(t) + y_n(t). \qquad (A.3)$$

Substituting Eq. (A.3) into Eq. (A.1) and linearizing the resulting equation yield

$$\frac{d^2 y_n(t)}{dt^2} = a\left[V'(h)\sum_{l=1}^{p}\beta_l(y_{n+l}-y_{n+l-1}) - \frac{dy_n(t)}{dt}\right] + \sum_{j=1}^{q}\kappa_j\left(\frac{dy_{n+j}(t)}{dt} - \frac{dy_{n+j-1}(t)}{dt}\right), \quad (A.4)$$

where

$$V'(h) = \left.\frac{dV(\Delta x_n)}{d\Delta x_n}\right|_{\Delta x_n = h}.$$

Expanding $y_n(t)$ in the Fourier-modes, i.e.,

$$y_n(t) = \exp(i\theta n + i\omega t),$$

where $\theta = 2\pi k/N$, $(k=0,1,\cdots,N-1)$, N is the total car number. We obtain

$$\omega^2 + a\left(V'\sum_{l=1}^{p}\beta_l\exp(i\theta)(1-\exp(-i\theta)) - i\omega\right) + i\omega\sum_{j=1}^{q}\kappa_j\exp(i\theta j)(1-\exp(-i\theta)) = 0. \quad (A.5)$$

In the following, we study the condition under which Eq. (A.5) has real valued solution ω. Let $a_c(\theta)$ be the critical value of a, such that three different cases of the Fourier-mode $\exp(i\theta n + i\omega t)$ can be classified, i.e., for $a = a_c(\theta)$ the mode is marginal $(\Im\omega(\theta) = 0)$, for $a > a_c(\theta)$ the mode is stable $(\Im\omega(\theta) > 0)$ and for $a = a_c(\theta)$ the mode is unstable $(\Im\omega(\theta) < 0)$.

The real part and imaginary part of Eq. (A.5) can be given as

$$\omega^2 - \omega\sum_{j=1}^{q}\kappa_j\Big(\sin(\theta j) - \sin\theta(j-1)\Big) + a_c(\theta)V'\sum_{l=1}^{p}\beta_l\Big(\cos(\theta l) - \cos\theta(l-1)\Big) = 0, \quad (A.6)$$

$$\omega a_c(\theta) - \omega\sum_{j=1}^{q}\kappa_j\Big(\cos(\theta j) - \cos\theta(j-1)\Big) - a_c(\theta)V'\sum_{l=1}^{p}\beta_l\Big(\sin(\theta l) - \sin\theta(l-1)\Big) = 0. \quad (A.7)$$

Let $\kappa_j = \lambda_j/\tau = \lambda_j a$, $(j=0,1,\cdots,q)$. It follows from Eqs. (A.6) and (A.7) that Eqs. (3.1) and (3.2) can be obtained.

The system is stable if and only if $a > a_c(\theta)$. From numerical calculations for Eq. (3.1) in the case of Eqs. (3.3) and (3.4), it can be found that $a_c(\theta)$ has maximum value at $\theta \to 0$. The longest wave-length mode is most unstable in this case. Thus the neutral stable line can be given by (3.5) and the stability condition of the system can also be given by (3.6).

B   Appendix to Section 4

Substituting Eqs. (4.1)-(4.3) into Eq. (4.4), and making the Taylor expansions to the fifth order of ε, we obtain the following nonlinear partial differential equation:

$$\varepsilon^2(b-V')\partial_X R + \varepsilon^3\left[\frac{b^2}{a} - \frac{1}{2}V'\sum_{l=1}^{p}\beta_l(2l-1) - \sum_{j=1}^{q}\left(\kappa_j\frac{b}{a}\right)\right]\partial_X^2 R$$

$$+\varepsilon^4\left\{\partial_T R + \left[-\frac{1}{6}V'\sum_{l=1}^{p}\beta_l\left(3l^2-3l+1\right) - \frac{1}{2}\sum_{j=1}^{q}\left(\kappa_j(2j-1)\frac{b}{a}\right)\right]\partial_X^3 R - \frac{1}{6}V'''\partial_X R^3\right\}$$

$$+\varepsilon^5\left\{\left(\frac{2b}{a} - \sum_{j=1}^{q}\frac{\kappa_j}{a}\right)\partial_X R\partial_T R + \left[-\frac{1}{24}V'\sum_{l=1}^{p}\beta_l(4l^3-6l^2+4l-1)\right.\right.$$

$$\left.\left. -\frac{1}{24}\sum_{j=1}^{q}\kappa_j\left((3j^2-3j+1)\frac{b}{a}\right)\right]\partial_X^4 R - \frac{1}{12}V'''\sum_{l=1}^{p}\beta_l(2l-1)\partial_X^2 R^3\right\} = 0, \quad (B.1)$$

where

$$V' = \frac{dV(\Delta x_n)}{d\Delta x_n}\bigg|_{\Delta x_n = h_c} = V'(h_c), \quad V''' = \frac{d^3 V(\Delta x_n)}{d\Delta x_n^3}\bigg|_{\Delta x_n = h_c} = V'''(h_c).$$

Near the critical point (h_c, a_c), with $b = V'$, $a_c = (1 + \varepsilon^2 a)$, where

$$a_c = \left(2V'(h_c) - 2\sum_{j=1}^{q}\kappa_j\right)\Bigg/\left(\sum_{l=1}^{p}\beta_l(2l-1)\right),$$

Eq. (B.1) can be simplified as

$$\varepsilon^4\left[\partial_T R - g_1\partial_X^3 R + g_2\partial_X R^3\right] + \varepsilon^5\left[g_3\partial_X^2 R + g_4\partial_X^4 R + g_5\partial_X^2 R^3\right] = 0, \qquad (B.2)$$

where $g_1, \cdots, g_5$ are given by (4.8). In order to get the standard mKdV equation, we use the transformations

$$T' = g_1 T, \quad R = \sqrt{\frac{g_1}{g_2}}R'. \qquad (B.3)$$

Substituting Eq. (B.3) into Eq. (B.2), we obtain the regularized equation

$$\partial_T R' - \partial_X^3 R' + \partial_X R'^3 + \varepsilon M[R'] = 0, \qquad (B.4)$$

where $M[R']$ is given by (4.6). Eq. (B.4) is the modified KdV equation with an $o(\varepsilon)$ correction term.

References

[1] D. Chowdhury, L. Santen and A. Schadschneider, Statistical physics of vehicular traffic and some related systems, Phys. Rep., 329 (2000), 199-329.
[2] D. Helbing, Traffic and related self-driven many-particle systems, Rev. Mod. Phys., 73 (2001), 1067.
[3] M. Bando, K. Hasebe, A. Nakayama, A. Shibata and Y. Sugiyama, Dynamical model of traffic congestion and numerical simulation, Phys. Rev. E, 51 (1995), 1035.
[4] D. Helbing and B. Tilch, Generalized force model of traffic dynamics, Phys. Rev. E, 58 (1998), 133.
[5] R. Jiang, Q. S. Wu and Z. J. Zhu, Full velocity difference model for a car-following theory, Phys. Rev. E, 64 (2001), 017101.
[6] Y. Xue, L. Y. Dong, Y. W. Yuan and S. Q. Dai, Numerical simulation on traffic flow with the consideration of relative velocity, Acta Phys. Sin., 51 (2002), 492 (in Chinese).
[7] Y. Xue, A car-following model with stochastically considering the relative velocity in a traffic flow, Acta Phys. Sin., 52 (2003), 2750 (in Chinese).
[8] T. Nagatani, Stabilization and enhancement of traffic flow by the next-nearest-neighbor interaction, Phys. Rev. E, 60 (1999), 6395.
[9] A. Nakayama, Y. Sugiyama, K. Hasebe, Effect of looking at the car that follows in an optimal velocity model of traffic flow, Phys. Rev. E, 65 (2001), 016112.
[10] H. Lenz, C. K. Wagner and R. Sollacher, Multi-anticipative car-following model, Eur. Phys. J. B, 7 (1999), 331.

[11] K. Hasebe, A. Nakayama and Y. Sugiyama, Dynamical model of a cooperative driving system for freeway traffic, Phys. Rev. E, 68 (2003), 026102.

[12] H. X. Ge, S. Q. Dai, L. Y. Dong and Y. Xue, Stabilization effect of traffic flow in an extended car-following model based on an intelligent transportation system application, Phys. Rev. E, 70 (2004), 066134.

[13] H. X. Ge, S. Q. Dai and L. Y. Dong, An extended car-following model based on intelligent transportation system application, Physica A, 365 (2006), 543-548.

[14] H. X. Ge, R. J. Cheng and S. Q. Dai, KdV and kink-antikink solitons in car-following models, Physica A, 357 (2005), 466-476.

[15] T. Wang, Z. Y. Gao and X. M. Zhao, Multiple velocity difference model and its stability analysis, Acta Phys. Sin., 55 (2006), 634 (in Chinese).

[16] D. A. Kurtz and D. C. Hong, Traffic jams, granular flow, and soliton selection, Phys. Rev. E, 52 (1995), 218-221.

[17] T. S. Komatsu, S. Sasa, Kink soliton characterizing traffic congestion, Phys. Rev. E, 52 (1995), 5574.

[18] T. Nagatani, Modified KdV equation for jamming transition in the continuum models of traffic, Physica A, 261 (1998), 599-607.

[19] T. Nagatani, Jamming transitions and the modified Korteweg-de Vries equation in a two-lane traffic flow, Physica A, 265 (1999), 297-310.

[20] P. Ioannou and M. Stefanovic, Evaluation of ACC vehicles in mixed traffic: lane change effects and sensitivity analysis, IEEE Trans. Intell. Transp. Syst., 6(1) (2005), 79-89.

[21] L. C. Davis, Effect of adaptive cruise control systems on traffic flow, Phys. Rev. E, 69 (2004), 066110.

[22] Z. P. Li and Y. C. Liu, Analysis of stability and density waves of traffic flow model in an ITS environment, Eur. Phys. J. B, 53 (2006), 367-374.